A Fourier-synthesis custom-coherence illuminator for EUV microfield lithography

Patrick Naulleau[1], Kenneth A. Goldberg[1], Phil Batson, Jeffrey Bokor[1,2], Paul Denham[1], and Senajith Rekawa[1]

[1]Center for X-Ray Optics, Lawrence Berkeley National Laboratory, Berkeley, CA 94720
[2]EECS Department, University of California, Berkeley, CA 94720

Abstract

Scanning illumination systems provide for a powerful and flexible means for controlling illumination coherence properties. Here we present a scanning Fourier synthesis illuminator that enables microfield EUV lithography to be performed on an intrinsically coherent synchrotron undulator beamline. The effectiveness of the system is demonstrated through a variety of print experiments, including the use of resolution enhancing coherence functions enabling the printing of 50-nm line-space features using a lithographic optic with a numerical aperture of 0.1 and an operational wavelength of 13.4 nm.

OCIS Codes: 030.1640, 070.2580, 110.4980, 110.5220, 110.7440, 120.4820, 120.5800, 220.3740, 260.7200, 340.6720, 340.7440

Introduction

The successful development of extreme ultraviolet (EUV) lithography[1] can be greatly aided through the deployment of flexible, microfield lithography test beds. Although not under serious consideration for manufacturing applications, synchrotron radiation provides a convenient well-characterized debris-free source for such microfield systems. The problem with synchrotron radiation, however, is the poor match between its intrinsic coherence properties and those required of a lithographic tool. Although particularly true for undulator radiation,[2] this statement also holds for bend-magnet radiation.

In general, meaningful lithography studies require the illumination coherence area to be only slightly larger than the diffraction-limited resolution of the lithographic optic. In the parlance of lithography, the illumination coherence factor (σ) is typically chosen to be approximately 0.7, where σ is often described as the ratio of the illumination divergence to the lithographic optic object-side numerical aperture (NA). Under the condition where an incoherent source is imaged to the lithographic optic object plane (*critical* illumination) using a so-called condenser lens, this ratio can be seen as the ratio of the condenser NA to the lithographic optic entrance NA. In terms of coherence area, the true metric of interest, a coherence factor of 0.7 would correspond to the diffraction-limited resolution of the lithographic optic being 0.7 times as large as the illumination coherence diameter.

In addition to simply achieving a specific σ value, advanced EUV lithography studies would greatly benefit from a controllable coherence factor as well as the ability to produce unconventional coherence functions. Here we present the implementation of a scanning illuminator capable of *in-situ* coherence function control at EUV wavelengths and demonstrate

its capabilities using a state-of-the-art 0.1-NA lithographic optic[3] and nominally coherent undulator radiation.

Coherence control

By way of the Wiener-Khinchin theorem,[4] it is well known that there exists a Fourier transform relationship between spectral bandwidth and temporal coherence. Similarly, the Van Citter-Zernike theorem[4] can be interpreted as specifying an equivalent Fourier transform relationship between spatial bandwidth and spatial coherence in the illumination plane. In order to control spatial coherence, we thus need to control spatial bandwith.

At visible wavelengths, a particularly common method for controllably reducing spatial coherence is to use a random phase modulator conveniently implemented as rotating ground glass.[5,6] When such a system is used as the effective source in a Köhler illuminator (the source is in the back focal plane of the condenser lens), the illumination coherence can be controlled by setting the size and/or shape of the illumination spot on the ground glass. By virtue of the effective source being in the back focal plane of the condenser lens, the spatial-frequency spectrum of the illumination emerging from the condenser will be directly related to the effective source size. Such a system is impractical at EUV wavelengths, however, due to the difficulties involved in obtaining equivalent random phase modulators.

An alternative coherence-control method, more suitable to EUV applications, involves a scanning process.[7,8] In this method, the desired illumination spatial-frequency spectrum is effectively synthesized through the scanning process. Spectral Fourier synthesis is a well-known technique for both spatial and temporal coherence control. It has been used in the past to implement various coherence-imaging techniques such as lensless imaging,[9] imaging through scattering media,[10] and direct image transmission through optical fibers.[11]

In a Fourier synthesis scanning illuminator such as the one shown in Fig. 1, a coherent beam (or any beam with a higher degree of coherence than desired) is scanned through a range of angles to produce a desired spatial-frequency spectrum. The individual spatial-frequency components are mutually incoherent (as is required for coherence synthesis) by virtue of the components not coexisting in time. Assuming, the observation, or image integration, time to be long relative to the scan rate, it can be shown that the coherence properties of the illumination produced by this system will be indistinguishable from that of a traditional source with the same spatial spectrum.[7-11] Heuristically, this can be explained by noting that for calculation purposes, partially-coherent imaging is often treated as an incoherent summation of coherent images produced under plane wave illumination over a range of angles.

An alternative description of the functionality of the Fourier synthesis illuminator can be presented from the point of view of the lithographic concept of pupil fill. Under typical lithographic circumstances, the coherence factor described above can be directly visualized by observing the illumination pattern in the pupil (the pupil fill). For the effectively *critical* illumination system described here, the lithographic optic pupil can be viewed as a Fourier-transform plane of the source, thus observing the pupil reveals the source spatial-spectral content. Scanning the source serves to paint out the pupil fill with a small dot representing the intrinsic coherence (or pupil fill) obtained without scanning. Again, it is evident that the illumination coherence properties (or pupil fill) can be synthesized through a source-scanning pattern.

As stated above, the coherence control achieved with this system assumes the observation time to be long relative to the scan rate. In practice this means that the lithographic exposure time should be at least as long as it takes to fully scan the desired pupil fill once. Additionally, the

exposure time should be constrained to an integer multiple of the full pupil fill scan time. If this condition is not satisfied, some portions of the pupil fill would receive higher weighting than others, thereby changing the coherence properties relative to the desired pupil fill.

Implementation at EUV

The Fourier synthesis concept described above has been used to implement a custom coherence illuminator for an EUV microstepper implemented at an undulator beamline at Lawrence Berkeley National Laboratory's Advanced Light Source synchrotron radiation facility. This undulator beamline has previously been demonstrated to intrinsically provide illumination of nearly complete spatial coherence.[12] Figure 1 shows a schematic of the Fourier-synthesis scanning illumination system. The undulator beam is nominally collimated and the scanning mirror is re-imaged to the reticle (mask) plane using a spherical mirror. Taking the scanning mirror to be the new effective source, this illuminator can be viewed as a *critical* illuminator (the source is imaged to the object). We note that this system is not restricted to being implemented to provide *critical* illumination. For example, if the incoming beam is focused to a plane that is re-imaged by the spherical mirror to the lithographic optic pupil and this plane is considered to be the effective source plane, then the scanning mirror can be viewed as synthesizing the source size instead of the source spectrum. Additionally, this would now be recognized as a Köhler system. We note, however, that these distinctions are somewhat arbitrary given that the extended source in either case is virtual.

The scanning-synthesis illuminator described here need not be limited to single scanning and condenser elements as presented here, but could be comprised of multi-element scanning and/or condenser systems. Moreover, dual-domain illuminators can be created allowing both the effective source size and the effective source spatial bandwidth to be synthesized.

For the implementation described here, the multilayer-coated spherical imaging mirror is placed 100 mm below the object plane and is illuminated at an angle of 5.4 degrees from normal. The coating parameters are chosen to match the lithographic optic wavelength while operating at an angle of 5.4 degrees. The scanning mirror is positioned 335 mm above the spherical mirror, yielding a reduction ratio of approximately 3.35 from the effective source to the reticle. The imaging condition requires the mirror radius of curvature to be 155 mm. The illumination size at the reticle is nominally 400 μm in diameter as set by the beamline-determined illumination size on the scanning mirror in conjunction with the factor of 3.35 reduction from the scanner to the reticle.

Because the reduction ratio has an inverse effect on angle, the angle range required of the scanning mirror is 3.35 times smaller than the angular range sought at the reticle. To achieve a σ of up to 1 with a 0.025-NA (object side) imaging optic, the required maximum deflection is 0.025/3.35 = 7.5 mrad (~0.4°). Given the distance from the scanning mirror to the spherical mirror, supporting this σ requires the spherical mirror to have a diameter of approximately 5 mm or larger.

We note that due to the ~45° orientation of the scanning mirror, the magnitudes of the actual mirror tilts must be different in the two directions to achieve uniform deflection in the two directions. Mirror tilts orthogonal to the plane of incidence must be approximately sqrt(2) larger to achieve the same angular deflection as do mirror tilts aligned with the plane of incidence.

The complete microstepper optical path is depicted in Fig. 2. The reflective reticle is imaged to a resist-coated wafer using a 0.1-NA, four-mirror, 4×-reduction, lithographic optic. This state-of-the-art optic[13,14] is the second of two optical systems fabricated as part of an industry consortium (the EUV LLC) effort developing EUV lithography in collaboration with

Lawrence Berkeley, Lawrence Livermore, and Sandia National laboratories. Following static microfield characterization using the system described here, the lithographic optic will be installed into the fully-functional EUV lithography engineering test stand (ETS), an alpha-class stepper.[15]

Figure 3 shows a series of EUV pupil fills generated by the Fourier synthesis system described here. The images were recorded using a back-thinned back-illuminated EUV CCD camera positioned to capture the projection of the lithographic optic pupil. The black background represent the full 0.1-NA optic pupil. These images demonstrate the wide variety of pupil fills (coherence functions) that can be generated, including resolution enhancing pupil fills such as dipole illumination. An important benefit of the variable pupil-fill capability is the ability to model pupil fills used in other systems. For example, the final image in Fig. 3 shows pupil-fill generated with the scanning system set to emulate the 6-Channel pupil fill used in the actual ETS stepper. This level of control allows the system presented here to characterize the imaging performance of the lithographic optic under conventional illumination conditions as well as investigating pupil-fill specific effects arising from unconventional pupil fills.

As described above, achieving the desired coherence properties with the scanning system requires the exposure time to be at least as long as it takes to synthesize the desired pupil fill once. In the case of a typical $\sigma = 0.7$ pupil fill, the full pupil scan time is approximately 1 second limited by the mechanical resonance of the 2-D scanner. In practice we cycle through the pupil fill at least four times for improved uniformity; thus, a typical exposure is 4 seconds long. We note that were the scan time not a limiting factor, the undulator beamline would have enough power to support millisecond exposures in the 100-μm diameter printed microfield. In the

present condition, the beamline power is intentionally restricted. We note that this is not a fundamental limitation and that a faster scanner could readily be developed.

Print-based demonstration of coherence control

The static exposure system described above has been used to characterize the imaging performance of the ETS Set-2 optic, a 0.1-NA optic intended for 100-nm critical dimensions (CD) at an operational wavelength of 13.4 nm.[3] At the center of the field, where all subsequent printing results are presented, the optic was interferometrically measured to have a 37-Zernike-term wavefront figure quality of 0.69 nm or 52 mwaves.[13] Here we present imaging results particularly relevant to the functionality of the illuminator; more complete analyses of the imaging performance of the Set-2 optic itself have been published elsewhere.[16,17]

Figure 4 shows a series of images recorded with the scanning illumination system turned off. As evidenced by the coherent artifacts, essentially fully coherent imaging is attained ($\sigma \approx 0$). Figure 4(a) shows 100-nm features in focus, where relatively good imaging performance is achieved at this CD. Moving out of focus by 1.5 μm, however, Fig. 4(b) shows the same 100-nm features demonstrating severe ringing effects. Figure 4(c) shows 70-nm features in focus, which corresponds very closely to the coherent cut-off of the 0.1-NA optic. As expected, the 70-nm features are barely resolved under coherent illumination.

Figure 5 contains a similar set of images, but this time with the scanning illuminator turned on to produce nominally disk-fill illumination with $\sigma = 0.8$. Like Figs. 4(a) and (c), Figs. 5(a) and (b) show in-focus images of 100-nm and 70-nm features, respectively. Figure 5(c) shows the 70-nm features 0.6-μm out of focus. Dramatic improvement in imaging quality is achieved both in terms of coherent artifact elimination and improved resolution as demonstrated by the 70-nm features.

As described above, the implementation of the custom-coherence illuminator enables the resolution of the system to be enhanced through the use of specialized pupil fills, such as dipole illumination (Fig. 3). By breaking the pupil fill into two poles, the resolution is improved in the pole-separation direction at the expense of resolution in the orthogonal direction. Figure 6 shows printed images with dipole illumination where the pole separation is set to enhance vertical lines. The 70-nm elbows in Fig. 6(a) demonstrate the resolution loss in the horizontal direction. Figures 6(b) and (c) show 60 and 50 nm lines and spaces, respectively. For comparison purposes, Fig. 6(d) shows the 50-nm line-space pattern printed using conventional disk illumination with a σ of 0.8. As expected, dipole illumination has significantly improved the resolution of the system. The 50-nm equal line-space pattern represents a k_1 factor of 0.37, where k_1 is defined as $(CD)(NA)/\lambda$. We note that the conventional Rayleigh resolution criterion corresponds to a k_1 factor of 0.61 and a CD of 82 nm for this optic.

Another important benefit of the scanning illuminator is its ability to simulate system-specific pupil fills such as the unique ETS 6-channel pupil fill (Fig. 3). Although good performance is achieved down to 70-nm for certain orientations using the ETS pupil fill,[15,16] Fig. 7 shows that increased horizontal-vertical bias limits the ability to print 70-nm scale features in *Manhattan* geometry (vertical and horizontal features only). Figures 7(a) and (b) compare Manhattan geometry 70-nm elbows printed using ETS and disk pupil fills ($\sigma = 0.7$), respectively. Printing results show a horizontal-vertical bias of 16.2 nm for the ETS pupil fill and 8.8 nm for the disk fill. Part of the bias present in the ETS-fill case, and the majority of the bias present in the disk-fill case, can be attributed to bias on the mask combined with a mask shadowing effect caused by off-normal mask illumination in a direction orthogonal to the horizontal features. Both these effects could, in principle, be mitigated through the use of a properly biased mask.

Summary

A scanning Fourier synthesis illuminator, operating at EUV wavelengths, has been developed allowing intrinsically coherent sources (such as synchrotron undulator sources) to be used for developmental microfield lithography. This system enables relatively simple illuminator design when using sources of higher coherence than desired for lithography, or other imaging applications. Moreover, the flexibility of the coherence synthesis method allows the illuminator to generate arbitrary coherence functions or pupil fill. This system has been implemented at Lawrence Berkeley National Laboratory's Advanced Light Source synchrotron radiation facility to lithographically characterize a diffraction-limited 0.1-NA EUV lithographic optic. Using this system, 50-nm line-space printing has been demonstrated, corresponding to a k_1 factor of 0.37, where the Rayleigh limit corresponds to a k_1 factor of 0.61.

Acknowledgements

The authors are greatly indebted to Kevin Bradley, Rene Delano, Gideon Jones, David Richardson, and Ronald Tackaberry for expert engineering and fabrication support, to Farhad Salmassi and Keith Jackson for lithography and print-analysis support, and to the entire CXRO staff for enabling this research. This research was supported by the Extreme Ultraviolet Limited Liability Company and the DOE Office of Basic Energy Science.

References

1. R. Stulen and D. Sweeney, "Extreme ultraviolet lithography," IEEE J. Quantum Electron. **35**, 694-699 (1999).
2. D. Attwood, G. Sommargren, R. Beguiristain, K. Nguyen, J. Bokor, N. Ceglio, K. Jackson, M. Koike, and J. Underwood, "Undulator radiation for at-wavelength interferometry of optics for extreme-ultraviolet lithography," Appl. Opt. **32**, 7022-7031 (1993).
3. D. W. Sweeney, R. Hudyma, H. N. Chapman, and D. Shafer, "EUV optical design for a 100 nm CD imaging system," in *Emerging Lithographic Technologies II*, Y. Vladimirsky, ed., Proc. SPIE **3331**, 2-10 (1998).
4. J. W. Goodman, *Statistical Optics*, John Wiley & Sons, New York, 1986, **Chap. 5**, 157-229.
5. M. V. R. K. Murty, "Interference between wave fronts rotated or reversed with respect to each other and its relation to spatial coherence," J. Opt. Soc. Am. **54**, 1187-1190 (1964).
6. W. Martienssen and E. Spiller, "Coherence and Fluctuations in Light Beams," Am. J. Phys. **32**, 919-926 (1964).
7. K. Itoh and Y. Ohtsuka, "Illumination with a moving light source," Opt. Comm. **31**, 119-124 (1979).
8. K. Itoh and Y. Ohtsuka, "Coherence control by laser scanning," Appl. Opt. **19**, 3184-3188 (1980).
9. E. Arons and D. Dilworth, "Lensless imaging by spatial Fourier synthesis holography," Appl. Opt. **35**, 777-781 (1996).
10. E. Arons and D. Dilworth, "Analysis of Fourier synthesis holography for imaging through scattering media," Appl. Opt. **34**, 1841-1847 (1995).

11. P. Naulleau, "Analysis of the confined-reference coherence-encoding method for image transmission through optical fibers," Appl. Opt. **36**, 7386-7396 (1997).
12. C. Chang, P. Naulleau, E. Anderson, and D. Attwood, "Spatial coherence characterization of undulator radiation," Opt. Comm. **182**, 24-34 (2000).
13. K. Goldberg, P. Naulleau, J. Bokor, and H. Chapman, "Honing the accuracy of extreme ultraviolet optical system testing: at-wavelength and visible-light measurements of the ETS Set-2 projection optic," Proc. SPIE Vol. **4688**, *to be published* (2002).
14. P. Naulleau, K. Goldberg, E. Anderson, P. Batson, P. Denham, S. Rekawa, and J, Bokor, "At wavelength characterization of the Engineering Test Stand Set-2 optic," J. Vac. Sci. & Technol. B **19**, 2396-2400 (2001).
15. D. Tichenor, A. Ray-Chaudhuri, S. Lee, H. Chapman, W. Replogle, K. Berger, R. Stulen, G. Kubiak, L. Klebanoff, J. Wronosky, D. O'Connell, A. Leung, K. Jefferson, W. Ballard, L. Hale, K. Blaedel, J. Taylor, J. Folta, E. Spiller, R. Soufli, G. Sommargren, D. Sweeney, P. Naulleau, K. Goldberg, E. Gullikson, J. Bokor, D. Attwood, U. Mickan, R. Hanzen, E. Panning, P. Yan, J. Bjorkholm, and C. Gwyn, "Initial Results from the EUV Engineering Test Stand," Proc. SPIE Vol. **4506**, 639-645 (2001).
16. P. Naulleau, K. Goldberg, E. Anderson, D. Attwood, P. Batson, J. Bokor, P. Denham, E. Gullikson, B. Hoef, K. Jackson, S. Rekawa, F. Salmassi, K. Blaedel, H. Chapman, L. Hale, R. Soufli, E. Spiller, D. Sweeney, J. Taylor, C. Walton, G. Cardinale, A. Ray-Chaudhuri, A. Fisher, G. Kubiak, D. O' Connell, R Stulen, D. Tichenor, C. Gwyn, P. Yan, G. Zhang, "Static microfield printing at the Advanced Light Source with the ETS Set-2 optic," Proc. SPIE **Vol. 4688**, *to be published* (2002).

17. P. Naulleau, K. Goldberg, E. Anderson, D. Attwood, P. Batson, J. Bokor, P. Denham, E. Gullikson, B. Harteneck, B. Hoef, K. Jackson, D. Olynick, S. Rekawa, F. Salmassi, K. Blaedel, H. Chapman, L. Hale, P. Mirkarimi, R. Soufli, E. Spiller, D. Sweeney, J. Taylor, C. Walton, D. O' Connell, R. Stulen, D. Tichenor, C. Gwyn, P. Yan and G. Zhang, "Sub-70-nm EUV Lithography at the Advanced Light Source Static Microfield Exposure Station Using the ETS Set-2 Optic," *submitted to J. Vac. Sci. & Technol. B* (2002).

List of Figures

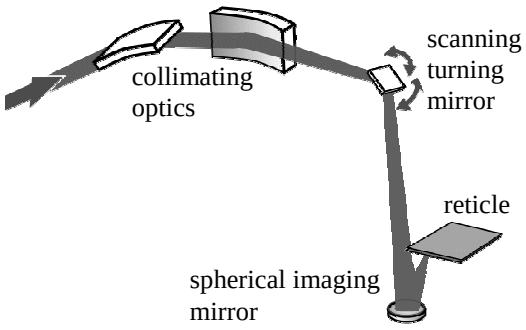

Fig. 1. Schematic of scanning Fourier-synthesis illuminator. A 2-D angle scanning turning mirror serves as an effective source that is re-imaged to the reticle using a spherical mirror. The spatial bandwidth (coherence) of the effective source is synthesized through the scanning process.

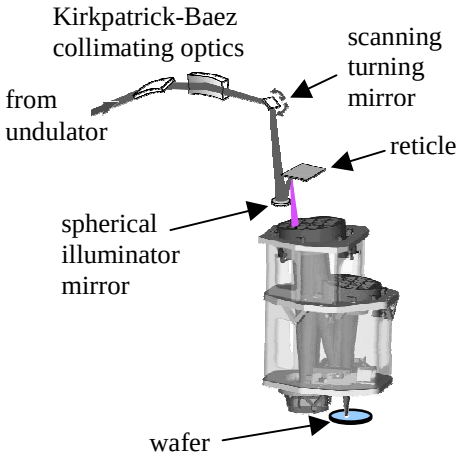

Fig. 2. Schematic of microfield static printing system.

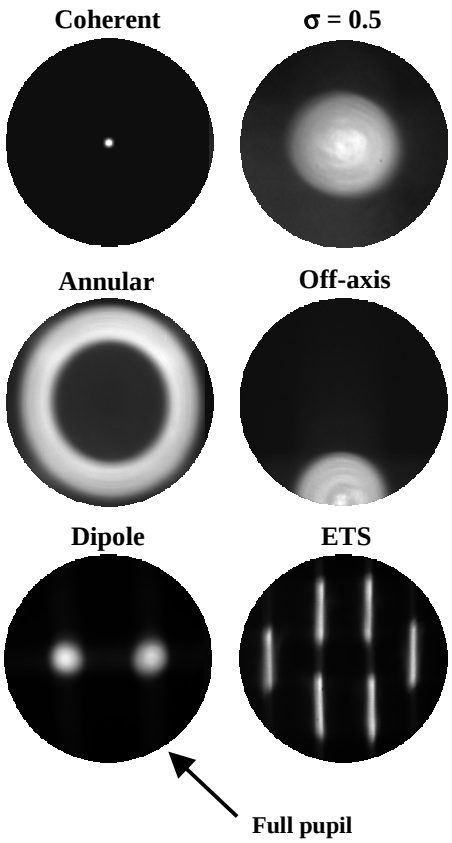

Fig. 3. Series of EUV pupil fills generated by the scanning system described above and recorded through the lithographic ETS Set-2 optic. A back-thinned back-illuminated EUV CCD camera is used to capture the pupil-fill images.

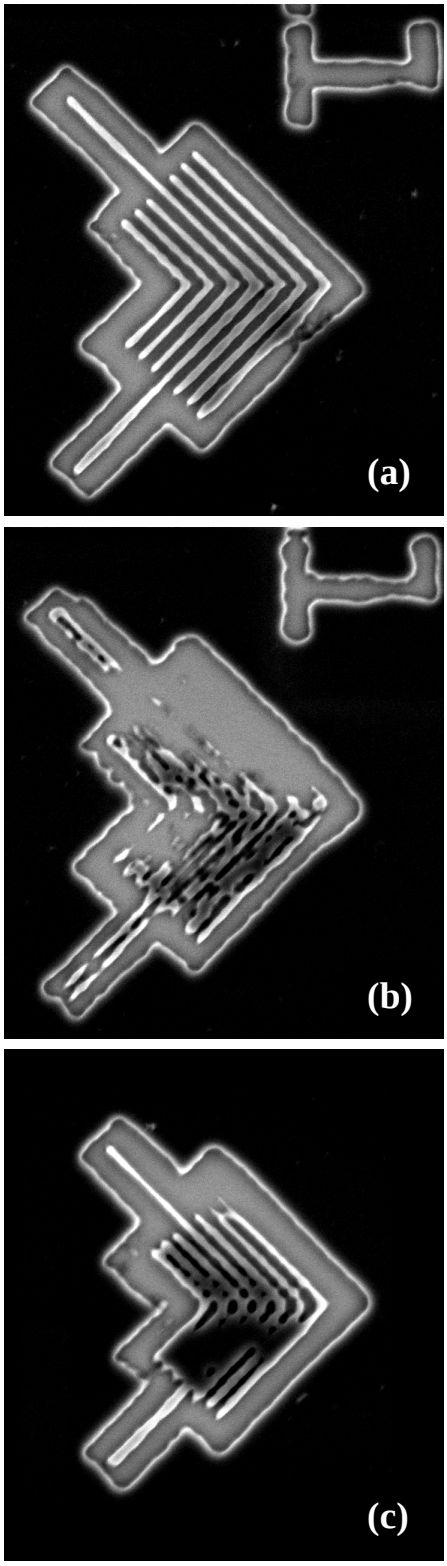

Fig. 4. Coherent images ($\sigma \approx 0$) obtained with scanning system turned off. (a) 100-nm line-space pattern in focus. (b) 100-nm line-space pattern 1.5 μm out of focus. (c) 70-nm line-space pattern in focus.

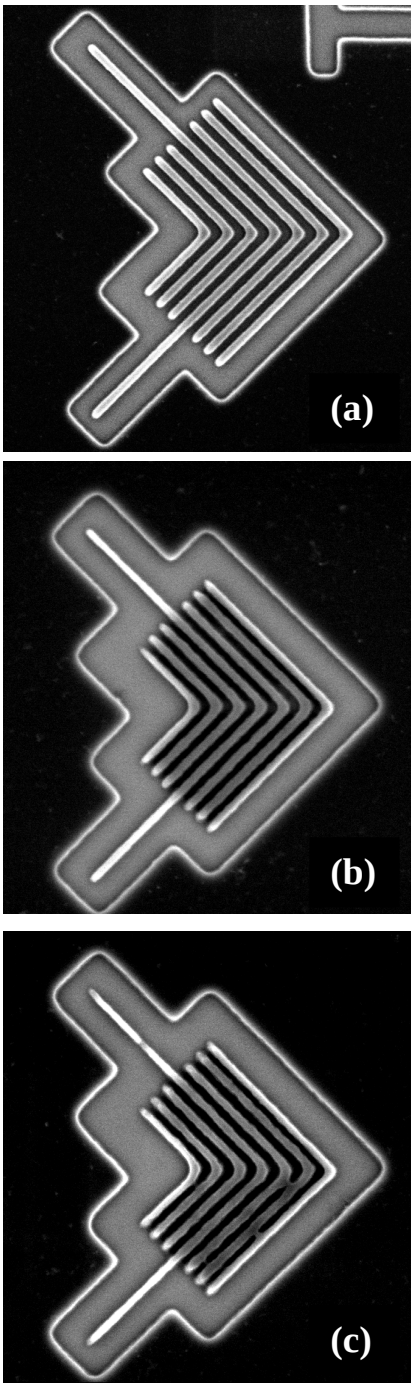

Fig. 5. Partially coherent images with disk fill ($\sigma = 0.8$) obtained with scanning system turned on. (a) 100-nm line-space pattern in focus. (b) 70-nm line-space pattern in focus. (c) 70-nm line-space pattern 0.6 μm out of focus.

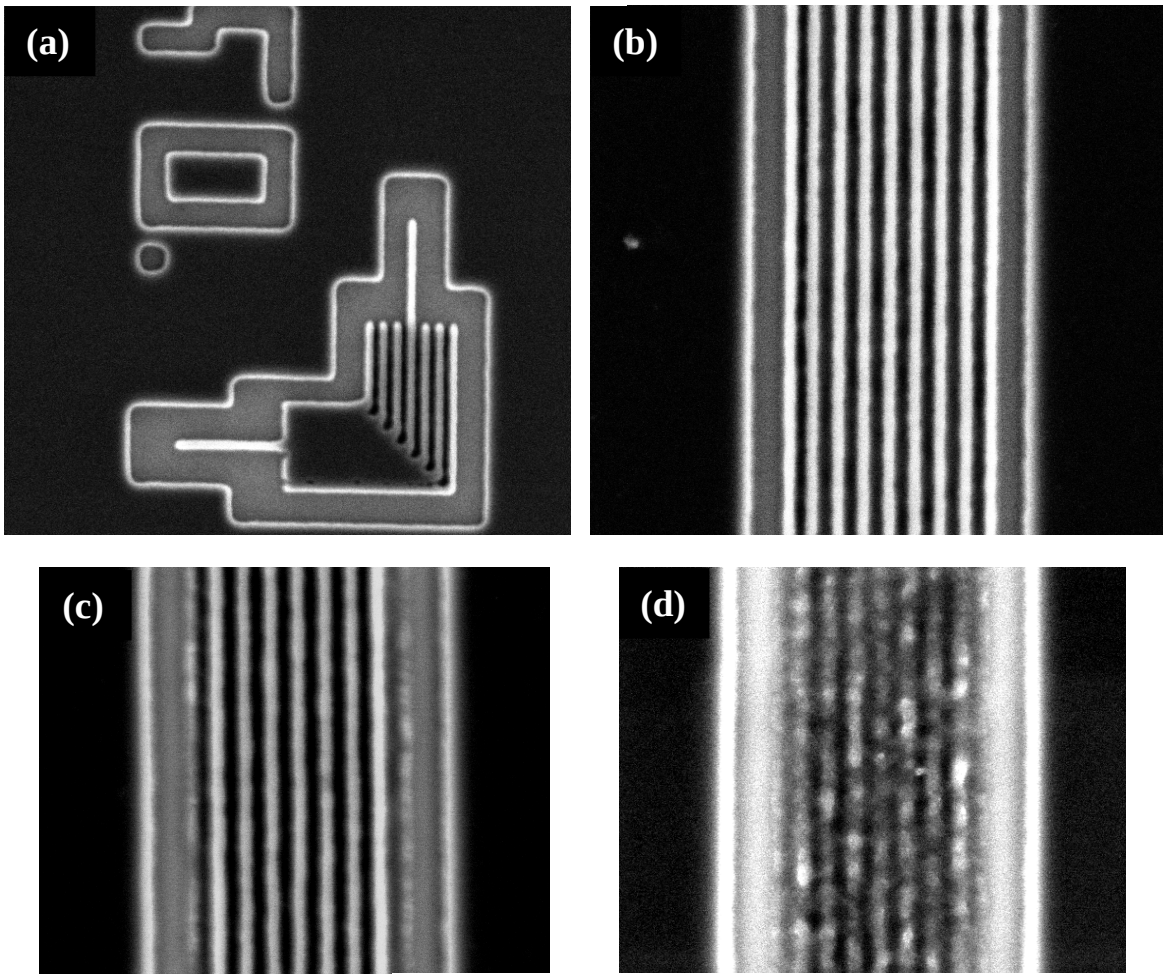

Fig. 6. (a)-(c) show printing results with dipole illumination where the pole separation is set to enhance vertical lines. (a) 70-nm elbows demonstrating the resolution loss in the horizontal direction. (b) 60-nm line-space pattern. (c) 50-nm line-space pattern. For comparison purposes (d) shows the 50-nm line-space pattern printed using conventional disk illumination with a σ of 0.8.

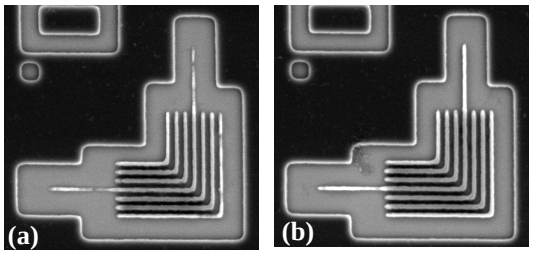

Fig. 7. Comparison Manhattan geometry 70-nm elbows printed using ETS (a) and disk (b) pupil fills ($\sigma = 0.7$).